Available online at www.sciencedirect.com
ScienceDirect
Trans. Nonferrous Met. Soc. China 22(2012) 373−379
Transactions of Nonferrous Metals Society of China
www.tnmsc.cn

Synthesis and upconversion luminescence of Lu_2O_3:Yb^{3+},Tm^{3+} nanocrystals

LI Li[1, 2], CAO Xue-qin[2], ZHANG You[1], GUO Chang-xin[2]

1. College of Mathematics and Physics, Chongqing University of Posts and Telecommunications, Chongqing 400065, China;
2. Department of Physics, University of Science and Technology of China, Hefei 230026, China

Received 21 January 2011; accepted 22 September 2011

Abstract: Lutetium oxide nanocrystals codoped with Tm^{3+} and Yb^{3+} were synthesized by the reverse-like co-precipitation method, using ammonium hydrogen carbonate as precipitant. Effects of the Tm^{3+}, Yb^{3+} molar fractions and calcination temperature on the structural and upconversion luminescent properties of the Lu_2O_3 nanocrystals were investigated. The XRD results show that all the prepared nanocrystals can be readily indexed to pure cubic phase of Lu_2O_3 and indicate good crystallinity. The experimental results show that concentration quenching occurs when the mole fraction of Tm^{3+} is above 0.2%. The optimal Tm^{3+} and Yb^{3+} doped molar fractions are 0.2% and 2%, respectively. The strong blue (490 nm) and the weak red (653 nm) emissions from the prepared nanocrystals were observed under 980 nm laser excitation, and attributed to the $^1G_4\rightarrow{}^3H_6$ and $^1G_4\rightarrow{}^3F_4$ transitions of Tm^{3+}, respectively. Power-dependent study reveals that the $^1G_4$ levels of Tm^{3+} can be populated by three-step energy transfer process. The upconversion emission intensities of 490 nm and 653 nm increase gradually with the increase of calcination temperature. The enhancement of the upconversion luminescence is suggested to be the consequence of reducing number of OH^- groups and the enlarged nanocrystal size.

Key words: Lu_2O_3:Yb^{3+},Tm^{3+} nanocrystal; co-precipitation method; upconversion luminescence

1 Introduction

In recent years, upconversion luminescence of lanthanide-doped nanocrystals have attracted much attention due to their unique optical properties and potential applications in such fields as infrared to visible upconversion lasers, fibre amplifiers, color displays, optical communications and biological fluorescencelabels [1−3]. Many trivalent rare earth ions, such as Er^{3+} [4], Tm^{3+} [5] and Pr^{3+} [6], are doped as emission and absorption centres in these materials. Among the rare earth ions, Yb^{3+} becomes the most suitable sensitizer ion because of its special energy levels and long excited level lifetime. Tm^{3+} is a promising optical activator that opens the possibility for simultaneous blue and ultraviolet emission of laser action and various applications [7]. When a rare earth-doped optical device is developed, the host material is a very important factor to be considered. The host material with low phonon energy can result in a reduction of the multiphonon relaxation and help efficient upconversion occur. Therefore, choosing an appropriate host is very important for obtaining highly efficient upconversion luminescence. Rare earth oxides, as promising hosts for upconversion, possess relatively low phonon energy, high chemical durability and favorable physical properties [8]. During the past few years, extensive studies have been concentrated on the upconversion luminescence of Y_2O_3 host [9, 10]. The sesquioxide Lu_2O_3 is isostructural to Y_2O_3 and crystallizes in a cubic bixbyite structure. Lutetium could be a more favorable cation for RE^{3+} ions dopant emission [11]. Additionally, Yb^{3+} (86 pm) and Tm^{3+} (87 pm) have ionic radii similar to Lu^{3+} (85 pm), in favor of the dopant substitution. Therefore, Lu_2O_3 is an ideal host for the upconversion luminescent materials.

Co-precipitation method is one of the most promising techniques because of its advantages, such as the relatively simple synthetic route, low cost and ease of mass production. Although there are only some reports on the upconversion of rare earth ions-doped Lu_2O_3

Foundation item: Projects (10704090, 10774140, 11047147) supported by the National Natural Science Foundation of China; Projects (KJ090514, KJTD201016) supported by the Natural Science Foundation of Chongqing Municipal Education Commission, China
Corresponding author: LI Li; Tel: +86-23-62471721; E-mail: lilic@cqupt.edu.cn; lilic@mail.ustc.edu.cn
DOI: 10.1016/S1003-6326(11)61186-2

nanocrystals [12−14], there is no systematic study on the effect of Tm^{3+} content and calcination temperature on the structural and upconversion luminescent properties of Lu_2O_3:Yb^{3+},Tm^{3+} nanocrystals. In this work, lutetium oxide nanocrystals codoped with Tm^{3+} and Yb^{3+} were synthesized by a reverse-strike co-precipitation method. The effects of Tm^{3+}, Yb^{3+} molar fractions and calcination temperature on the structure and the upconversion emission intensity of the Lu_2O_3:Yb^{3+},Tm^{3+} nanocrystals were investigated. The upconversion mechanisms were also discussed.

2 Experimental

Lu_2O_3 nanocrystals codoped with 2% Yb^{3+} (molar fraction, the same below) and 0.04%, 0.2%, 0.5%, 1%, and 2% Tm^{3+} were prepared by the reverse-like co-precipitation method, respectively. High pure Lu_2O_3 (99.99%), Yb_2O_3 (99.99%) and Tm_2O_3 (99.99%) were used as starting materials and ammonium hydrogen carbonate (NH_4HCO_3, A. R., 1 mol/L solution) was precipitant. Aqueous nitrate solutions were prepared by dissolving Lu_2O_3, Yb_2O_3 and Tm_2O_3 in HNO_3 (A. R.) and distilled water under stirring and heating. The respective nitrate solutions were mixed with an appropriate proportion. The mixed salt solution was then added drop by drop to the excess NH_4HCO_3 solution at a speed of 2 mL/min under vigorous stirring at room temperature. After the process of titration, the precipitate was aged for 2 h with agitation by a electric stirrer to make the reaction proceed sufficiently. After filtering and washing with distilled water and anhydrous ethanol several times, the precipitates were dried at 80 °C for 12 h in an oven. The precipitates were further calcined in air at 900 °C for 2 h to obtain nanocrystals. Moreover, Lu_2O_3 nanocrystals codoped with 0.2% Tm^{3+} and 1%, 2%, 4%, 6%, 10%, and 15% Yb^{3+} were synthesized by the same procedure, respectively.

To investigate the effect of calcination temperature on the upconversion luminescence of Lu_2O_3:2% Yb, 0.2% Tm nanocrystals, the nanocrystals were obtained by calcining the precipitates at 800, 900, 1000 and 1100 °C for 2 h, respectively, using the same procedure.

The crystal structures were analyzed by a MXPAHF rotating anode X-ray diffractometer with Cu K_α radiation (λ=0.154056 nm). The morphology of nanocrystals was examined on a FEI-Sirion 200 field-emission scanning electron microscope. The FT-IR transmittance spectra were recorded in the range of 400−4000 cm^{-1} on a Magna-IR 750 Fourier transformation infrared spectrometer. The upconversion luminescence spectrum was detected by R955 (Hamamatsu) from 400 to 700 nm, using an 980 nm diode laser Module (K98D08m−30W, China) as the excitation source. The excitation power was 455 mW. All spectra were collected at room temperature.

3 Results and discussion

3.1 Influence of Tm^{3+} molar fraction on structural and upconversion luminescent properties for Lu_2O_3:2%Yb^{3+}, $x$$Tm^{3+}$ nanocrystals

Figure 1 shows the XRD patterns of Lu_2O_3 nanocrystals doped with 2% Yb^{3+} and x Tm^{3+}(x=0.04%, 0.2%, 0.5%, 1%, 2%) and calcined at 900 °C and the data of JCPDS card No. 43−1021 for Lu_2O_3 were used as a reference. The patterns indicate that the nanocrystals were crystallized as cubic Lu_2O_3 with spatial group *Ia*3(206). No additional peaks of other phases have been found, indicating that the RE^{3+} ions are effectively doped into the host lattice. The high intensity of the diffraction peaks indicates good crystallinity of the nanocrystals. The average crystalline sizes can be estimated by using Scherrer equation [15]:

$$D=\frac{0.89\lambda}{\beta\cos\theta} \tag{1}$$

where λ stands for the wavelength of Cu K_α radiation; β is the corrected full width at half maximum (FWHM) of the diffraction peak; θ denotes the diffraction angle; 0.89 is the characteristic of spherical particle. Using the Scherrer equation, the estimated crystalline size of Lu_2O_3: Yb^{3+}, Tm^{3+} nanocrystals is 40−60 nm.

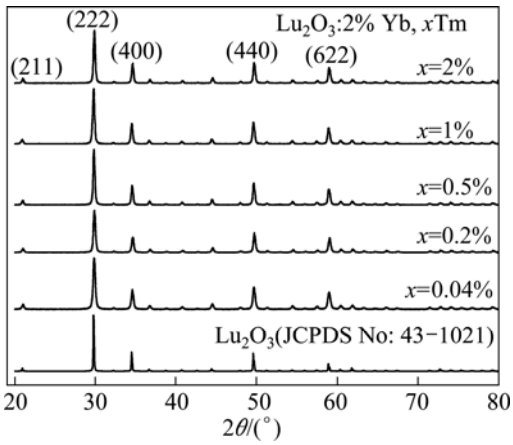

Fig. 1 XRD patterns of Lu_2O_3 nanocrystals doped with 2% Yb^{3+} and 0.04%, 0.2%, 0.5%, 1%, 2% Tm^{3+} and calcined at 900 °C and compared with standard pattern of JCPDS 43−1021

Figure 2 presents the typical FE-SEM image of Lu_2O_3:2% Yb^{3+}, 0.2% Tm^{3+} nanocrystals calcined at 900 °C. As shown in Fig. 2, the obtained Lu_2O_3:2% Yb^{3+}, 0.2% Tm^{3+} nanocrystals are aggregated, and have nearly spherical shape and an average diameter of 60 nm, which are consistent with the XRD results. The similar results were also observed for other Lu_2O_3:Yb^{3+}, Tm^{3+}

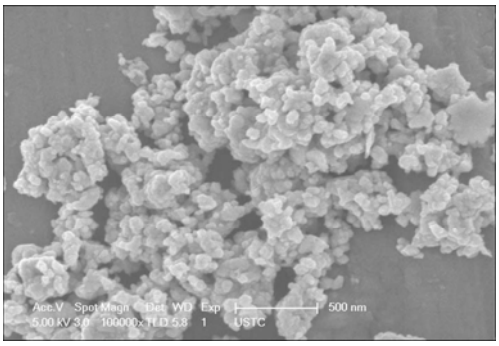

Fig. 2 FE-SEM image of Lu_2O_3:2% Yb^{3+}, 0.2% Tm^{3+} nanocrystals

nanocrystals with various contents of Tm^{3+} (not shown here).

The typical upconversion spectrum of the Lu_2O_3:2% Yb^{3+}, 0.2% Tm^{3+} nanocrystals calcined at 900 °C and excited by 980 nm diode laser excitation at room temperature is shown in Fig. 3. The strong blue emission around 490 nm easily seen by naked eye is assigned to the $^1G_4 \rightarrow {}^3H_6$ transition of Tm^{3+}. Weak red emission around 653 nm is attributed to the $^1G_4 \rightarrow {}^3F_4$ transition. The experimental results show that the upconversion emission intensity ratio of the blue to red is approximately equal to 12 for the Lu_2O_3:2% Yb^{3+}, 0.2% Tm^{3+}nanocrystals.

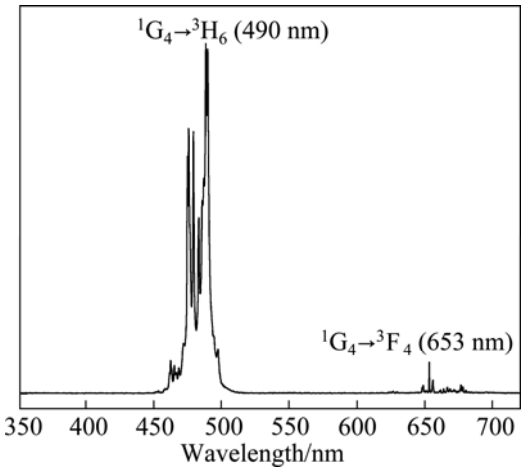

Fig. 3 Upconversion emission spectrum of Lu_2O_3:2% Yb^{3+}, 0.2% Tm^{3+} nanocrystals calcined at 900 °C under 980 nm excitation

Figure 4 shows the upconversion emission intensity of Lu_2O_3 nanocrystals doped with 2% $Yb^{3+}$and $x$$Tm^{3+}$ and calcined at 900 °C as a function of Tm^{3+} content. As shown in Fig. 4, with increasing the Tm^{3+} content, the upconversion emission intensity increases at first, reaching a maximum value with 0.2% Tm^{3+} and then gradually decreases at higher doping concentrations. Concentration quenching occurs above 0.2% dopant content. When Tm^{3+} content is high, the self-quenching or cross-relaxation mechanisms between Tm^{3+} ions becomes active [16−18]. The energy transfer processes can be described as follows:

$$Tm^{3+}(^1G_4)+Tm^{3+}(^3H_6)\rightarrow Tm^{3+}(^3F_2)+Tm^{3+}(^3F_4)$$

$$Tm^{3+}(^1G_4)+Tm^{3+}(^3H_6)\rightarrow Tm^{3+}(^3H_4)+Tm^{3+}(^3H_5)$$

$$Tm^{3+}(^3H_4)+Tm^{3+}(^3H_6)\rightarrow Tm^{3+}(^3F_4)+Tm^{3+}(^3F_4)$$

which can depopulate the$^1G_4$ levels but populate the $^3H_5$ levels, leading to an increase in the extent of non-radiative transitions. Moreover, host may transfer the energy to lattice defects discussed later, which may trap energy, resulting in concentration quenching.

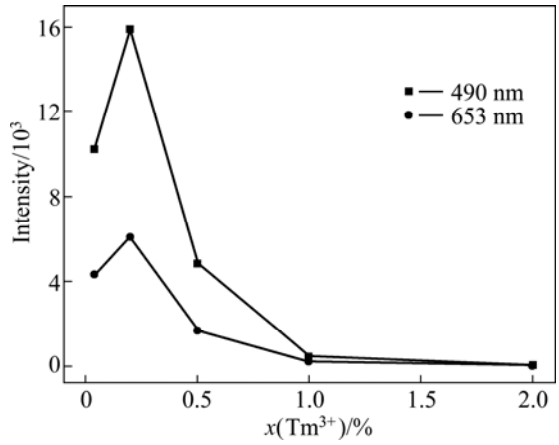

Fig. 4 Upconversion emission intensity of Lu_2O_3 nanocrystals doped with 2% Yb^{3+} and $x$$Tm^{3+}$ and calcined at 900 °C as function of Tm^{3+} mole fraction (The red emission intensity of 653 nm is magnified by a factor of 5)

3.2 Influence of Yb^{3+} molar fraction on structural and upconversion luminescent properties for Lu_2O_3:$x$$Yb^{3+}$, 0.2%$Tm^{3+}$ nanocrystals

Figure 5 shows the XRD patterns of Lu_2O_3 nanocrystals doped with 0.2% Tm^{3+} and x Yb^{3+}(x=1%, 2%, 4%, 6%, 10%, 15%) and calcined at 900 °C. The XRD results show that the diffracting peak positions of all the Lu_2O_3:$x$$Yb^{3+}$,0.2% Tm^{3+} nanocrystals are consistent with the standard powder diffraction pattern of Lu_2O_3 (JCPDS 43−1021). The crystalline size of Lu_2O_3: $x$$Yb^{3+}$, 0.2% Tm^{3+} nanocrystals is 40−60 nm using the Scherrer equation.

Figure 6 shows the upconversion emission intensity of Lu_2O_3 nanocrystals doped with 0.2% Tm^{3+} and $x$$Yb^{3+}$ and calcined at 900 °C as a function of Yb^{3+} content. It is noticed that the emission intensities of 490 nm and 653 nm first increase and approach a maximum at a doping content of 2% and then decrease with the increase of Yb^{3+} content. It is obvious that with the increase

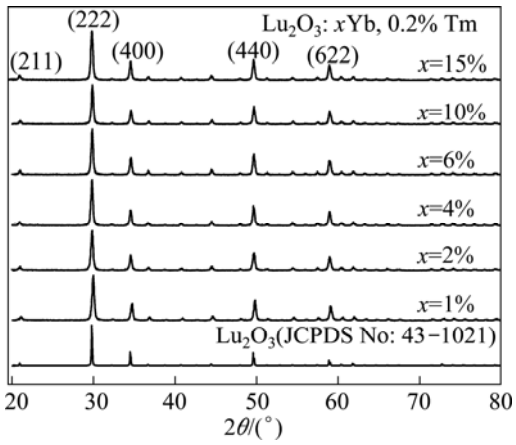

Fig. 5 XRD patterns of Lu_2O_3 nanocrystals doped with 0.2% Tm^{3+} and 1%, 2%, 4%, 6%, 10%, 15% Yb^{3+} and calcined at 900 °C and compared with standard pattern of JCPDS 43−1021

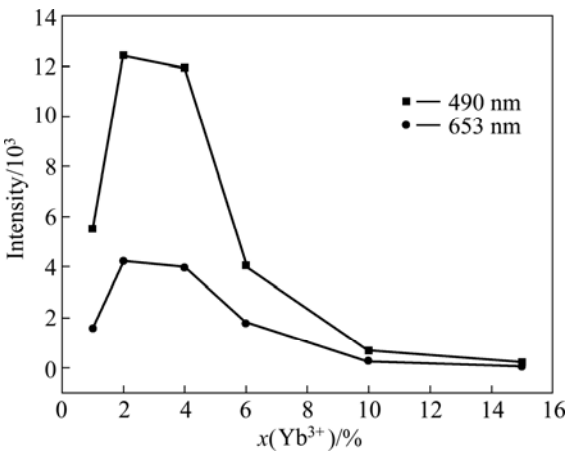

Fig. 6 Upconversion emission intensity of Lu_2O_3 nanocrystals doped with 0.2% Tm^{3+} and $x$$Yb^{3+}$ as function of Yb^{3+} mole fraction (The red emission intensity of 653 nm is magnified by a factor of 5)

of Yb^{3+} content, more energy is transferred from Yb^{3+} to Tm^{3+}. However, when Yb^{3+} ions are heavily doped, many factors such as increased amount of impunities, concentration-quenching of Yb^{3+}, energy back transfer from Tm^{3+} to Yb^{3+} can be described as $Tm^{3+}(^1G_4)+Yb^{3+}(^2F_{7/2})=Tm^{3+}(^3H_4)+Yb^{3+}(^2F_{5/2})$, which effectively reduces upconversion emission intensity.

3.3 Influence of calcination temperature on structural and upconversion luminescent properties for Lu_2O_3:2% Yb^{3+}, 0.2% Tm^{3+} nanocrystals

Figure 7 shows the XRD patterns of Lu_2O_3:2% Yb^{3+}, 0.2%Tm^{3+} nanocrystals calcined at various temperatures. The results reveal that all the prepared Lu_2O_3 nanocrystals are of cubic structure, and the diffracting peak positions are well consistent with the standard powder diffraction pattern of Lu_2O_3 (JCPDS 43−1021). The average crystalline size can be estimated by using Scherrer equation. In cubic crystal lattice [19], the lattice constant can be calculated from Eq. (2).

$$\frac{1}{d^2}=\frac{h^2+k^2+l^2}{a^2} \tag{2}$$

where d, a, and (h k l) are the interplanar distance, lattice constant and crystal indices (Miller indices), respectively. The strongest peaks (222) at 2θ=29.775, 29.812, 29.807, 29.806° and d=3.0010, 2.9962, 2.9967, 2.9961 Å were used to calculate the average crystallite size (D) and lattice constants (a) of the Lu_2O_3: 2% Yb^{3+}, 0.2% Tm^{3+} nanocrystals, respectively. Table1 presents the calculated crystallite sizes and lattice constants of Lu_2O_3:2% Yb^{3+}, 0.2% Tm^{3+} nanocrystals at different calcination temperatures. The lower the calcination temperature is, the smaller the crystallite sizes are. The crystallite size increases from 32 to 70 nm with the increase of calcination temperatures from 800 to 1100 °C. The lattice constants are compatible with the literature values (10.390 Å) from the standard card (JCPDS 43−1021).

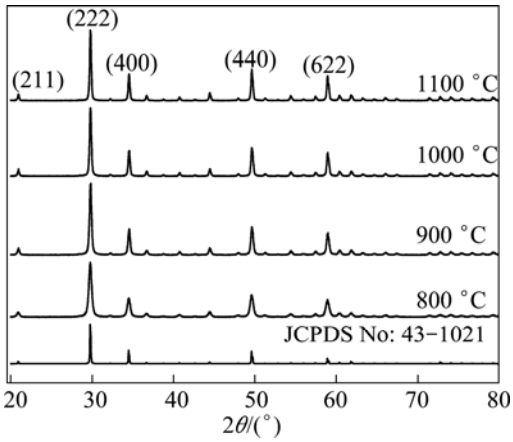

Fig. 7 XRD patterns of Lu_2O_3:2% Yb^{3+},0.2%Tm^{3+} nanocrystals calcined at various temperatures and compared with standard pattern of JCPDS 43−1021

Table 1 Calculated crystallite sizes and lattice constants of Lu_2O_3:2%Yb^{3+},0.2%Tm^{3+} nanocrystals calcined at various temperatures

Calcination temperature/°C	Crystallite size/nm	Lattice constant/Å
800	32	10.395
900	48	10.379
1000	63	10.381
1100	70	10.378

Figure 8 shows the FT-IR spectra of Lu_2O_3:2%Yb^{3+}, 0.2% Tm^{3+} nanocrystals calcined at various temperatures. The data show that the bands around 490 and 580 cm^{-1} are assigned to the Lu—O vibration of cubic Lu_2O_3 [20].

The absorption bands of OH^- (around 3400 cm^{-1}) become weaker with the increase of calcination temperature. OH^- groups with high vibration frequency will increase the nonradiative relaxation rate and hence decrease upconversion efficiency [21]. This indicates that the enhanced upconversion intensity may come from the reducing of OH^- groups, which are located on the surface of nanocrystals. From Table 1, it is known that the crystallite size of Lu_2O_3:2% Yb^{3+}, 0.2% Tm^{3+} nanocrystals increases with increasing the calcination temperature. The decrease of surface-to-volume ratio can reduce the OH^- groups on the surface of nanocrystals. Therefore, the reducing of OH^- groups is suggested to be relevant to the enhancement of the upconversion emission.

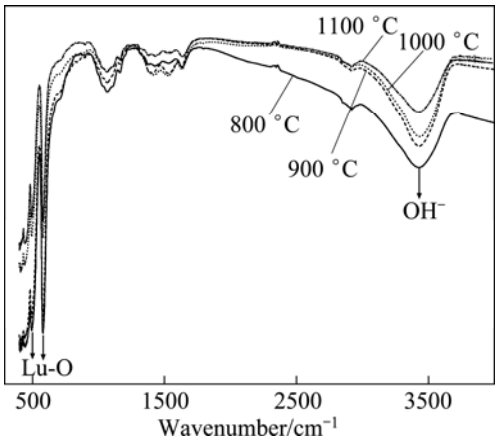

Fig. 8 FT-IR spectra of Lu_2O_3:2% Yb^{3+}, 0.2% Tm^{3+} nanocrystals calcined at various temperatures

Figure 9 shows the influence of calcination temperature on the upconversion emission intensity of 490 nm and 653 nm under 980 nm laser excitation. It can be seen that the emission intensities of 490 nm and 653 nm become stronger gradually with the increase of calcination temperature. The increased nanocrystal size can also contribute to the upconversion emission enhancement, since the larger nanocrystal size has less defects [22]. Larger Lu_2O_3:2% Yb^{3+}, 0.2% Tm^{3+} nanocrystals have lower surface-to-volume ratio which leads to lower surface scattering of the excitation light by the surface of the radiated Lu_2O_3 nanocrystals. As a result, the Lu_2O_3:2% Yb^{3+}, 0.2% Tm^{3+} nanocrystals with larger diameter can absorb more efficiently the excitation light than Lu_2O_3:2% Yb^{3+}, 0.2% Tm^{3+} nanocrystals with smaller diameter. It can be seen from Fig. 9 that the enhanced upconversion intensity may be due to the reduction of OH^- groups [23]. Therefore, the enhancement of the upconversion luminescence is suggested to be the consequence of reducing number of OH^- groups and the enlarged nanocrystal size.

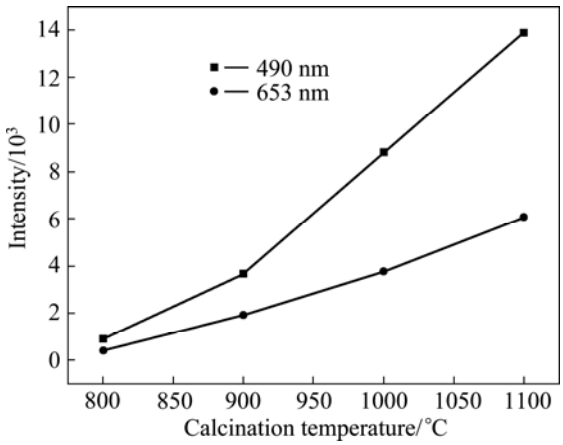

Fig. 9 Effect of calcination temperature on upconversion emission intensity of Lu_2O_3:2% Yb^{3+}, 0.2% Tm^{3+} nanocrystals (The red emission intensity of 653 nm is magnified by a factor of 5)

3.4 Upconversion mechanisms

The energy level diagram of Tm^{3+} and Yb^{3+} shown in Fig.10 can be used to explain the upconversion mechanism. The pump photons of 980 nm laser only excite Yb^{3+} ion, because Tm^{3+} ion has no matched excited level above its ground state. The upconversion emission intensity depends on the population of $^1G_4$ levels for Tm^{3+}, which can be populated by three-step process [24]. Under 980 nm laser excitation, the $^1G_4$ excited state can be populated by a three-step energy transfer (ET) process. Firstly, the $^2F_{7/2}\rightarrow{}^2F_{5/2}$ transition of Yb^{3+} occurs due to absorption of 980 nm photons. Then, Yb^{3+} in the $^2F_{5/2}$ level transfers its energy to Tm^{3+}, which is excited to the $^3H_5$ level and relaxes nonradiatively to

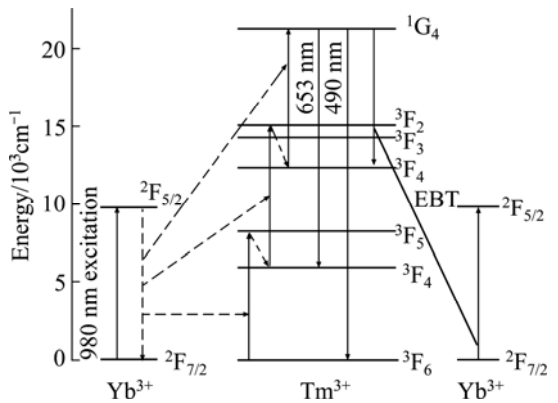

Fig. 10 Energy level diagram of Tm^{3+} and Yb^{3+} with excitation and emission process scheme (The full arrows pointing upwards represent energy absorption; full arrows pointing downwards represent emission; dotted arrows pointing downwards represent multiphonon relaxations (nonradiative decay); the diagonal line without arrows represents energy back transfer; dash-dotted arrows indicate energy transfer processes, respectively.)

the $^3F_4$ level. Tm^{3+} in the $^3F_4$ level can be excited to the $^3F_2$ level by energy transfer process after which nonradiative relaxation to $^3H_4$ occurs. Subsequently, Yb^{3+} in the $^2F_{5/2}$ level transfers its energy to Tm^{3+} and excites Tm^{3+} at $^3H_4$ level to $^1G_4$ level. Therefore, the Tm^{3+} decays radiatively to the $^3H_6$ ground state and the $^3F_4$ metastable state generating strong blue and weak red emissions around 490 nm and 653 nm from the $^1G_4$ levels, respectively.

The upconversion efficiency is principally governed by nonradiative processes in materials, which are dependent on the energy gap separating the upper and lower levels as well as the highest phonon energy in the materials. The multiphoton nonradiative decay rate can be expressed as [25]

$$W_n(T) = W_0(0)\left(\frac{\exp(h\nu / kT)}{\exp(h\nu / kT) - 1}\right)^n \quad (3)$$

where T is the absolute temperature; $W_n(T)$ is the rate at temperature T; $W_0(0)$ is the rate at 0 K; k is the Boltzmann constant; $n=\Delta E/(h\nu)$, n accounts for the number of phonons involved in the sensitizer excitation; $h\nu$ is the maximum phonon energy of the host matrix; ΔE is the energy gap involved. According to the energy gap law, multiphoton relaxation is dominant when $n<5$ [26]. The energy gap of Tm^{3+} between the levels $^1G_4$ and the $^3F_2$ is approximately equal to 5840 cm^{-1}, which corresponds to 9 phonons of the highest phonon energy (the maximum phonon energy of 600 cm^{-1} in our experiments), so the probability of non-radiative transition from the level $^1G_4$ to the level $^3F_2$ can be negligible. This indicates that high population at the level $^1G_4$ can be achieved.

To further understand the upconversion mechanisms, pump power (P_{pump}) dependences on the upconversion emission intensities (I_{up}) of Lu_2O_3:2% Yb^{3+},0.2% Tm^{3+} nanocrystals calcinated at 900 °C are shown in Fig. 11. According to the relationship between I_{up} and P_{pump}^n,

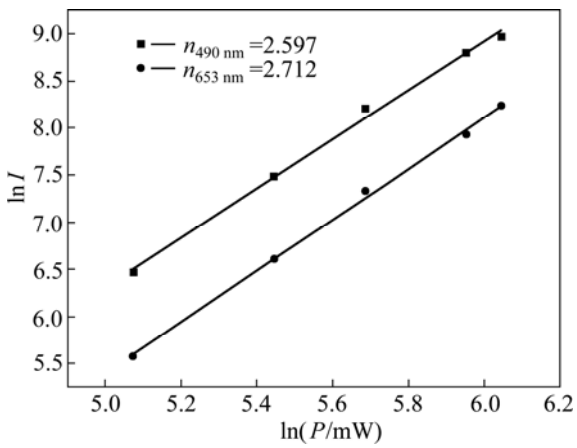

Fig. 11 Relationship between ln$I$ and ln$P$ of Lu_2O_3:2% Yb^{3+}, 0.2% Tm^{3+} nanocrystals under 980 nm excitation

where n is the number of photons involved in the pump process [27], the typical upconversion luminescent intensity I_{up} depends on the incident pump power P_{pump}. The upconversion emission intensities of Lu_2O_3:2% Yb^{3+}, 0.2% Tm^{3+}nanocrystals were integrated at 490 and 653 nm for various pump powers. A plot of ln I versus ln P yields a straight line with slope n. On the basis of the experimental data in Fig. 11, the obtained n values are 2.597 and 2.712. The two slopes are close to 3, which indicates that the blue and weak red upconversion luminescence is indeed a three-photon upconversion process.

4 Conclusions

1) The Lu_2O_3 nanocrystals codoped with 2% Yb^{3+} and 0.04%, 0.2%, 0.5%, 1%, 2% Tm^{3+} were successfully synthesized by the reverse-like co-precipitation method. The further investigation reveals that the upconversion emission intensity depends on the Tm^{3+} and Yb^{3+} contents and calcination temperature.

2) The experimental results show that all the prepared Lu_2O_3:2% Yb^{3+}, 0.2% Tm^{3+} nanocrystals can be readily indexed to pure cubic phase of Lu_2O_3. The strong blue and weak red emissions from the prepared nanocrystals were observed, and attributed to the $^1G_4 \rightarrow {}^3H_6$ and $^1G_4 \rightarrow {}^3F_4$ transitions of Tm^{3+} ion, respectively. Concentration quenching occurs when the content of Tm^{3+} is above 0.2%. Power-dependent study reveals that the $^1G_4$ level can be populated by three-step energy transfer process.

3) The upconversion emission intensities of 490 nm and 653 nm increase gradually with the increase of calcination temperature. The enhancement of the upconversion luminescence is suggested to be the consequence of reducing number of OH^- groups and the enlarged nanocrystal size.

4) The data presented in this study might provide useful information for further development of upconversion ceramic laser associated with the $^1G_4 \rightarrow {}^3H_6$ transitions of Tm^{3+} ions.

References

[1] LIU F, MA E, CHEN D Q, YU Y L, WANG Y S. Tunable red-green upconversion in novel transparent glass ceramics containing Er: $NaYF_4$ nanocrystals [J]. Journal of Physical Chemistry B, 2006, 110(42): 20843−20846.

[2] WANG M, MI C C, WANG W X, LIU C H, WU Y F, XU Z R, MAO C B, XU S K. Immunolabeling and NIR-excited fluorescent imaging of HeLa cells by using $NaYF_4$:Yb,Er upconversion nanoparticles [J]. ACS Nano, 2009, 3(6): 1580−1586.

[3] WANG F, LIU X G. Recent advances in the chemistry of lanthanide-doped upconversion nanocrystals [J]. Chemical Society Reviews, 2009, 38(4): 976−989.

[4] EILER H. Effect of particle/grain size on the optical properties of Y_2O_3:Er, Yb [J]. Journal of Alloys and Compounds, 2009, 474(1−2):

569−572.

[5] LIM K S, BABU P, LEE S K, PHAM V T, HAMILTON D S, Infrared to visible up-conversion in thulium and holmium doped lutetium aluminum garnet [J]. Journal of Luminescence, 2003, 102−103: 737−743.

[6] NACCACHE R, VETRONE F, SPEGHINI A, BETTINELLI M, CAPOBIANCO J A. Cross-relaxation and upconversion processes in Pr^{3+} singly doped and Pr^{3+}/Yb^{3+} codoped nanocrystalline $Gd_3Ga_5O_{12}$: The sensitizer/activator relationship [J]. Journal of Physical Chemistry C, 2008, 112(20):7750−7756.

[7] AN L Q, ZHANG J, LIU M, WANG S W. Upconversion luminescence of Tm^{3+} and Yb^{3+} codoped lutetium oxide nanopowders [J]. Journal of Alloys and Compounds, 2008, 451(1−2): 538−541.

[8] POLIZZI S, BUCELLA S, SPEGHINI A, VETRONE F, NACCACHE R, BOYER J C, CAPOBIANCO J A. Nanostructured lanthanide-doped Lu_2O_3 obtained by propellant synthesis [J]. Chemistry of Materials, 2004, 16(7): 1330−1335.

[9] BAI Y F, WANG Y X, PENG G Y, YANG K, ZHANG X R, SONG Y L. Enhance upconversion photoluminescence intensity by doping Li^+ in Ho^{3+} and Yb^{3+} codoped Y_2O_3 nanocrystals [J]. Journal of Alloys and Compounds, 2009, 478(1−2): 676−678.

[10] ZHANG Ming, LI Xin-ai, WANG Zhi-xing, HU Qi-yang, GUO Hua-jun. Synthesis of $Y_2O_3:Eu^{3+}$ phosphors by surface diffusion and their photoluminescence properties [J]. Transactions of Nonferrous Metals Society of China, 2010, 20: 115−118.

[11] CAPOBIANCO J A, VETRONE F, BOYER J C, SPEGHINI A, BETTINELLI M. Visible upconversion of Er^{3+} doped nanocrystalline and bulk Lu_2O_3 [J]. Optical Materials, 2002, 19(2): 259−268.

[12] FIORENZO V, BOYER J C, CAPOBIANCO J A. NIR to visible upconversion in nanocrystalline and bulk $Lu_2O_3:Er^{3+}$ [J]. Journal of Physical Chemistry B, 2002, 106(22): 5622−5628.

[13] AN L Q, ZHANG J, LIU M, WANG S W. Upconversion properties of Yb^{3+}, $Ho^{3+}:Lu_2O_3$ sintered ceramic [J]. Journal of Luminescence, 2007, 122−123: 125−127.

[14] YANG J, ZHANG C M, PENG C, LI C X, WANG L L, CHAI R T, LIN J. Controllable red, green, blue (RGB) and bright white upconversion luminescence of $Lu_2O_3:Yb^{3+}/Er^{3+}/Tm^{3+}$ nanocrystals through single laser excitation at 980 nm [J]. Chemistry-A European Journal, 2009, 15(18): 4649−4655.

[15] WANG C N, ZHAO J B, LI Y, ZHANG W P, YIN M. Influence of dispersant on $Y_2O_3:Eu^{3+}$ powders synthesized by combustion method [J]. Journal of Rare Earth, 2009, 27(6): 879−885.

[16] WANG X F, XIAO S G, BU Y Y, YANG X L, DING J W. β-$Na(Y_{1.5}Na_{0.5})F_6$: Tm^{3+}—A blue upconversion phosphor [J]. Journal of Luminescence, 2009, 129: 325−327.

[17] PEI X J, HOU Y B, ZHAO S L, ZHENG X, FENG T. Frequency upconversion of Tm^{3+} and Yb^{3+} codoped $YLiF_4$ synthesized by hydrothermal method [J]. Materials Chemistry and Physics, 2005, 90: 270−274.

[18] DEXTER D L, SCHULMAN J H. Theory of concentration quenching in inorganic phosphors [J]. The Journal of Physical Chemistry, 1954, 22(6): 1063−1070.

[19] JIA G, YOU H P, LIU K, ZHENG Y H, GUO N, ZHANG H J. Highly uniform Gd_2O_3 hollow microspheres: Template-directed synthesis and luminescence properties [J]. Langmuir, 2010, 26(7): 5122−5128.

[20] YANG J, LI C X, QUAN Z W, ZHANG C M, YANG P P, LI Y Y, YU C C, LIN J. Self-assembled 3D flowerlike Lu_2O_3 and $Lu_2O_3:Ln^{3+}$(Ln =Eu, Tb, Dy, Pr, Sm, Er, Ho, Tm) microarchitectures: Ethylene glycol-mediated hydrothermal synthesis and luminescent properties [J]. Journal of Physical Chemistry C, 2008, 112(33): 12777−12785.

[21] GUO H, DONG N, YIN M, ZHANG W P, LOU L R, XIA S D. Visible upconversion in rare earth ion-doped Gd_2O_3 nanocrystals [J]. Journal of Physical Chemistry B, 2004, 108(50): 19205−19209.

[22] VETRONE F, BOYER J C, CAPOBIANCO J A, SPEGHINI A, BETTINELLI M. Concentration-dependent near-infrared to visible upconversion in nanocrystalline and bulk $Y_2O_3:Er^{3+}$ [J]. Chemistry of Materials, 2003, 15(14): 2737−2743.

[23] CAPOBIANCO J A, VETRONE F, DALESIO T, TESSARI G., SPEGHINI A, BETTINELLI M. Optical spectroscopy of nanocrystalline cubic $Y_2O_3:Er^{3+}$ obtained by combustion synthesis [J]. Physical Chemistry Chemical Physics, 2000, 2(14): 3203−3207.

[24] QIN G S, QIN W P, WU C F, HUANG S H, ZHAO D, ZHANG J S, LU S Z. Intense ultraviolet upconversion luminescence from $Yb^{3+}$and Tm^{3+} codoped amorphous fluoride particles synthesized by pulsed laser ablation [J]. Optics Communication, 2004, 242(1−3): 215−219.

[25] CHEN G Y, LIU H C, LIANG H J, SOMESFALEAN G, ZHANG Z G. Upconversion emission enhancement in Yb^{3+}/Er^{3+}-codoped Y_2O_3 nanocrystals by tridoping with Li^+ ions [J]. Journal of Physical Chemistry C, 2008, 112: 12030−12036.

[26] WERMUTH M, RIEDENER T, GUDEL H U. Spectroscopy and upconversion mechanisms of $CsCdBr_3:Dy^{3+}$ [J]. Physical Review B, 1998, 57(8): 4369−4376.

[27] BALDA R, GARCIA-ADEVA A J, VODA M, FERNANDEZ J. Upconversion processes in Er^{3+}-doped KPb_2C_{15} [J]. Physical Review B, 2004, 69(20): 12030−12036.

$Lu_2O_3:Yb^{3+},Tm^{3+}$ 纳米晶的制备和上转换发光性能

李 丽[1,2], 曹雪琴[2], 张 友[1], 郭常新[2]

1. 重庆邮电大学 数理学院，重庆 400065；2. 中国科学技术大学 物理系，合肥 230026

摘 要：采用碳酸氢铵(NH_4HCO_3)为沉淀剂，用共沉淀法制备 Yb^{3+} 和 Tm^{3+} 共掺杂的 $Lu_2O_3:Yb^{3+},Tm^{3+}$纳米晶。研究 Tm^{3+} 摩尔分数、Yb^{3+}摩尔分数和煅烧温度对 $Lu_2O_3:Yb^{3+},Tm^{3+}$ 纳米晶的结构和上转换发光性能的影响。结果表明：所制备的纳米晶具有纯的 Lu_2O_3 相，结晶性较好。当掺杂的 Tm^{3+}浓度超过 0.2%(摩尔分数)时，出现浓度淬灭效应。Tm^{3+} 和 Yb^{3+}的最佳掺杂比分别为 0.2%和 2%(摩尔分数)。在 980 nm 半导体激光器的激发下，样品发射出蓝光(490 nm)和红光(653 nm)，分别对应 Tm^{3+}的 $^1G_4\rightarrow{}^3H_6$ 和 $^1G_4\rightarrow{}^3F_4$ 跃迁。发射强度与激发功率的关系表明，Tm^{3+} 的 $^1G_4$ 能级布居是三光子能量传递过程。随着煅烧温度的升高，上转换发光强度增强，这主要是因为随着温度的升高纳米晶表面的 OH^-减少和纳米晶尺寸增大。

关键词：$Lu_2O_3:Yb^{3+},Tm^{3+}$纳米晶；共沉淀法；上转换发光

(Edited by LI Xiang-qun)